

Impact of the spectral hardening of TeV cosmic rays on the prediction of the secondary positron flux

J. Lavalley^{1*†}

*Departamento de Física Teórica UAM & Instituto de Física Teórica UAM/CSIC
Universidad Autónoma de Madrid, Cantoblanco, 28049 Madrid — Spain*

2 June 2018

ABSTRACT

The rise in the cosmic-ray positron fraction measured by the PAMELA satellite is likely due to the presence of astrophysical sources of positrons, *e.g.* pulsars, on the kpc scale around the Earth. Nevertheless, assessing the properties of these sources from the positron data requires a good knowledge of the secondary positron component generated by the interaction of cosmic rays with the interstellar gas. In this paper, we investigate the impact of the spectral hardening in the cosmic-ray proton and helium fluxes recently reported by the ATIC2 and CREAM balloon experiments, on the predictions of the secondary positron flux. We show that the effect is not negligible, leading to an increase of the secondary positron flux by up to $\sim 60\%$ above ~ 100 GeV. We provide fitting formulae that allow a straightforward utilization of our results, which can help in deriving constraints on one’s favorite primary positron source, *e.g.* pulsars or dark matter.

Key words: Galactic cosmic rays; antimatter.

Preprint IFT-UAM/CSIC-10-77

1 INTRODUCTION

The increase in the positron fraction above a few GeV reported by the PAMELA collaboration (Adriani et al. 2009) has triggered a lot of interpretation attempts, but it is now likely that it is due to positrons originating from conventional astrophysical sources, like pulsars (*e.g.* Sturrock 1970; Shen 1970; Harding & Ramaty 1987; Boulares 1989; Aharonian et al. 1995; Chi et al. 1996; Profumo 2008; Malyshev et al. 2009; Yüksel et al. 2009; Delahaye et al. 2010) or SNRs (*e.g.* Berezhko et al. 2003; Blasi 2009), while some other spatial or solar effects might also play a role (*e.g.* Shaviv et al. 2009; Roberts 2010). These works have notably shown that a very few sources may dominate the high energy positron flux at the Earth, opening interesting perspectives for more accurate predictions in the near future (see Delahaye et al. 2010, for a detailed analysis). Nevertheless, these perspectives are based on the assumption that the secondary positron flux prediction is under control.

Secondary positrons originate from nuclear interactions of cosmic-ray nuclei with the interstellar gas, and

have been investigated into details by Moskalenko & Strong (1998), and more recently by Delahaye et al. (2009), who provided more insights on the theoretical uncertainties. Delahaye et al. (2010) have improved the predictions of the latter by including the Klein-Nishina corrections to the energy loss treatment. All these predictions rely on cosmic-ray nuclei spectra constrained from rather low energy data ($\lesssim 100$ GeV), which are mostly power laws. Nevertheless, two balloon experiments, ATIC2 (Panov et al. 2009) and CREAM (Ahn et al. 2010), have recently reported on a clear and almost concordant hardening in these spectra around a few TeV, with a very good statistics. Since high energy stable nuclei have quite long range propagation (*e.g.* Taillet & Maurin 2003), it is likely that this spectral inflection is not merely local and pertains over a few kpc scale around the Earth. Therefore, a consistent prediction of the secondary positron flux should take it into account.

In this paper, we study into detail the impact of these new cosmic ray measurements on the secondary positron flux predictions. We provide the reader with user-friendly fitting formulae which summarize our results, and which can be used to constrain any extra source of cosmic-ray positrons.

* E-mail: julien.lavalley@uam.es

† Multidark fellow

2 FROM THE HARDENING OF COSMIC-RAY NUCLEI SPECTRA TO THE HARDENING OF THE SECONDARY POSITRON SPECTRUM

2.1 Generalities

Predictions of secondary positrons are usually valid in the frame of a propagation model, which specifies the way the propagation equation is solved. For more insights on cosmic ray propagation, we refer the reader to *e.g.* Ginzburg & Syrovatskii (1964); Berezhinskii et al. (1990); Longair (1994). Here, we adopt the formalism described in Delahaye et al. (2010), where convection and diffusive reacceleration are neglected, which is known to be a good approximation in the GeV-TeV energy range (Delahaye et al. 2009), and where fully relativistic energy losses are considered. Aside from energy losses, our propagation ingredients are therefore the diffusion coefficient $K(E)$, that we take homogeneous, and the half-thickness L of the diffusion slab. We use sets of propagation parameters consistent with the analysis of the secondary-to-primary nuclei ratios performed by Maurin et al. (2001), and further used in Donato et al. (2004) to define the *minimal*, *median* and *maximal* sets widely used in the literature. We note that the *med* model, which was the best-fit model found in Maurin et al. (2001), has properties very similar to the best-fit model derived more recently in Putze et al. (2010) from a Markov chain Monte Carlo analysis. Details on the effects of these parameters on the electron and positron propagation are given in Delahaye et al. (2010). For the energy losses, we adopt the model denoted M1 in this reference.

Our whole propagation framework can be encoded in the form of a Green function $\mathcal{G}(E, \vec{x}_\odot \leftarrow E_s, \vec{x}_s)$ that characterizes the probability of a positron injected at any coordinate \vec{x}_s with energy E_s to reach an observer on Earth with energy $E \leq E_s$. This allows us to write the positron flux as the following convolution:

$$\phi(E) = \int_{\text{slab}} d^3 \vec{x}_s \int dE_s \mathcal{G}(E, \vec{x}_\odot \leftarrow E_s, \vec{x}_s) \mathcal{Q}(E_s, \vec{x}_s), \quad (1)$$

where \mathcal{Q} is the source term that we are going to determine in the following. For secondaries, it formally reads (*e.g.* Delahaye et al. 2009)

$$\mathcal{Q}(E, \vec{x}) = 4\pi \sum_{i,j} \int dE_k \phi_i(E_k) \frac{d\sigma_{ij}}{dE}(E_k \rightarrow E) n_j(\vec{x}), \quad (2)$$

where ϕ_i is the flux of a cosmic-ray species of index i , n_j is the interstellar density of a gas species of index j , and $d\sigma_{ij}$ is the inclusive nuclear cross section associated with the production of a positron of energy E from an ion of kinetic energy E_k . For the cosmic-ray nuclei and interstellar gas, we can safely consider the dominant species only, *i.e.* the protons and α ions on the one hand, and the hydrogen (90%) and helium (10%) gas on the other hand. As in Delahaye et al. (2009) we assume an overall gas density of $n_0 = 1 \text{ cm}^{-3}$ homogeneously distributed inside an infinite flat disk of half-thickness $h = 100 \text{ pc}$, such that $n_{\text{tot}}(\vec{x}) = 2h n_0 \delta(z)$, where z is the coordinate perpendicular to the Galactic plane. These values are justified either by measurements of the interstellar medium (Ferrière 2001) and the fact that high energy positrons have very short range propagation due to efficient energy losses — large scale fluctua-

tuations of the gas density have almost no effect on the local high energy positron flux.

2.2 The incident cosmic ray flux

In Delahaye et al. (2009), we solved Eqs. (1) and (2) assuming the proton and α fluxes as fitted in Shikaze et al. (2007) to the low energy BESS data (Sanuki et al. 2000; Wang et al. 2002; Haino et al. 2004). These fits are recalled hereafter:

$$\begin{aligned} \phi_p^{\text{bess}}(E_k) &= A \beta^{a_1} \left[\frac{\mathcal{R}}{1 \text{ GV}} \right]^{-a_2} \\ \phi_\alpha^{\text{bess}}(E_k/n) &= B \beta^{b_1} \left[\frac{\mathcal{R}}{1 \text{ GV}} \right]^{-b_2}, \end{aligned} \quad (3)$$

with $(A, a_1, a_2) = (1.94 \text{ cm}^{-2} \text{ s}^{-1} \text{ GeV}^{-1} \text{ sr}^{-1}, 0.7, 2.76)$ and $(B, b_1, b_2) = (0.71 \text{ cm}^{-2} \text{ s}^{-1} \text{ GeV}^{-1} \text{ sr}^{-1}, 0.5, 2.78)$, *i.e.* single power laws of indices $-a_2$ and $-b_2$, respectively, at high energy.

These functions are displayed (solid curves) in Fig. 1 together with the BESS (Sanuki et al. 2000; Wang et al. 2002; Haino et al. 2004; Shikaze et al. 2007), CAPRICE (Boezio et al. 1999, 2003), AMS01 (Aguilar et al. 2002), ATIC2 (Panov et al. 2006, 2009), and CREAM (Ahn et al. 2010) data — note that these data have been corrected for solar modulation effects (demodulated) by means of the Force Field approximation (Gleeson & Axford 1968; Fisk 1971), with Fisk potentials made explicit in the plot. It is clear that though these parameterizations provide reasonably good fits to the low energy data, they completely fail above a few tens of GeV. In particular, we can remark that the proton data (left panel) are overshoot between $\sim 10 \text{ GeV}$ and a few TeV, while the helium data (right panel) are underpredicted above $\sim 100 \text{ GeV/n}$. Moreover, though CREAM and ATIC2 seem to agree in their measurements of the helium flux, there is an unequivocal discrepancy in the proton flux.

Since the functions of Eq. (3) were used in Delahaye et al. (2009) and Delahaye et al. (2010) to improve the predictions of the secondary positron flux, it is worth revisiting these predictions again in light of the new cosmic ray data. For the inclusive nuclear cross sections, we still use the numerical approach presented in Kamae et al. (2006) for the proton-proton collision, with the correction prescriptions of Norbury & Townsend (2007) for nucleus-nucleus interactions. The change in the derivation of the positron source term defined in Eq. (2) will therefore only come from the updated fits of the proton and helium fluxes.

To illustrate the difference in the positron source term arising from considering either the CREAM or the ATIC2 proton data, we consider two different modelings defined by the preference we put in one or the other experiment. The proton flux parameterization will be the only change between these two cases, since the helium data of the two experiments are consistent and can be simultaneously fitted by the same function.

In the following, we denote F1p and F2p the parameterizations associated with the proton data, the former providing a good fit to the CREAM data, and the latter providing a good fit to the ATIC2 data. We also define a function F1He

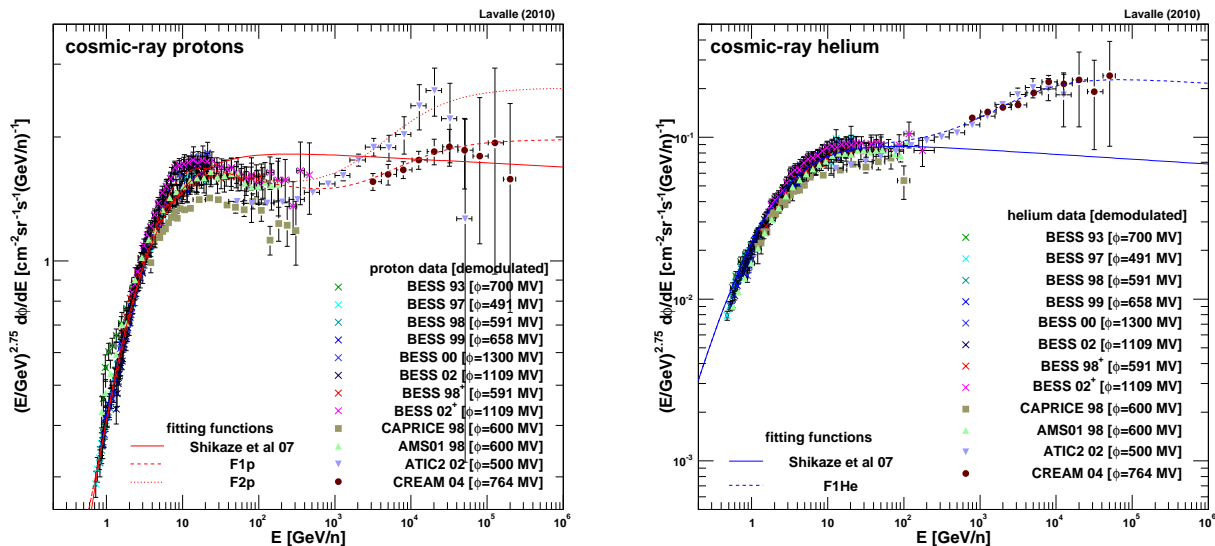


Figure 1. Left panel: cosmic-ray proton data. Right panel: cosmic-ray α data.

that provides a good fit to both CREAM and ATIC2 helium data. Functions F1p, F2p and F1He are given in Sec. 3.1, and are displayed in Fig. 1, in the left panel for the two first, and in the right panel for the last one. The functions of Eq. (3) will be referred to as *low energy fit*, or *reference fit*. In contrast, the combination of F1p and F1He will be referred to as *CREAM fit*, while F2p and FHe as *ATIC2 fit*.

2.3 Impact of the cosmic ray hardening on the secondary positron source term

In the left panel of Fig. 2, we derive the secondary positron source term defined in Eq. (2) and associated with the low energy fit (black curve), the CREAM fit (red curve), and the ATIC2 fit (blue curve); note that all of them run close to a power law in energy of index -2.7 . The contribution coming from the cosmic-ray proton is shown explicitly (dashed curves) for each modeling, as well as the α contribution (dotted curves). We see that the relative increase in the α contribution, from the low energy fit to F1He, is very large, reaching a factor of ~ 3 around a few TeV. Nevertheless, it remains subdominant with respect to the proton contribution. The difference in the proton flux modeling translates almost linearly into the positron source term, leading to a relative decrease with respect to the low energy fit below 100 GeV (1 TeV), and a relative increase above, for the ATIC2 (CREAM, respectively) fit. This comes from the fact that the inclusive cross section featuring in Eq. (2) scales like $\sim 1/E_k$ (Delahaye et al. 2009), straightforwardly leading to $Q \propto \phi_i(E_k)$; this explains why all contributions almost scale like $E^{-2.7}$. When summing up the contributions coming from proton and α interactions, we see that the relative decrease apparent in the proton-only case is less prominent due to the positive yield, though modest, of the α interactions: the net effect is a very slight decrease below 100 GeV, and a larger increase above. This is illustrated in more detail in the right panel of Fig. 2, where we plot the relative

difference of the CREAM (dashed curve) and ATIC2 (dotted curve) cosmic ray-induced positron source terms with the low energy reference case: the slight decrease below 100 GeV makes a 10% difference at most with the reference case, while the increase above reaches $\sim 30\%$ (60%) above a few TeV for the CREAM (ATIC2, respectively) configuration. The impact of using these new cosmic ray data is therefore not negligible in terms of secondary positron production.

2.4 Updated predictions for the secondary positron flux

Because of propagation, guessing the effect of the new cosmic ray modelings on the secondary positron flux prediction might not look, *a priori*, as straightforward as guessing their effect on the positron source term. This is formally due to the non-trivial dependence of the positron Green function on energy. We refer the reader to Delahaye et al. (2010), in particular to their Sect. 2.3, for more insights about this dependence. Nevertheless, since here we deal with a source term which is homogeneously distributed inside a thin disk of half-thickness h , and with an energy dependence close to a power law, we can assume that $Q(E, \vec{x} \approx 2h Q_0 \delta(z) (E/\text{GeV})^{-\tilde{\gamma}}$. In that case, the positron flux at the Earth can be approximated as (Delahaye et al. 2010):

$$\phi_{\odot}(E) \tilde{\propto} \frac{ch Q_0}{\sqrt{K_0/\tau_l}} (E/\text{GeV})^{-\tilde{\gamma}}, \quad (4)$$

where K_0 is the normalization of the diffusion coefficient, τ_l is the energy loss timescale, and $\tilde{\gamma} \approx \gamma + 0.5 (\alpha + \delta - 1)$ is the predicted flux spectral index which depends on the injected index γ and also on the diffusion coefficient index δ and the energy loss index α ($\alpha = 2$ in the Thomson approximation, but is < 2 when Klein-Nishina corrections become sizable).

The above equation is of great interest to anticipate the coming results, since it tells us that the ratio of two different flux predictions scales like the ratio of the corresponding

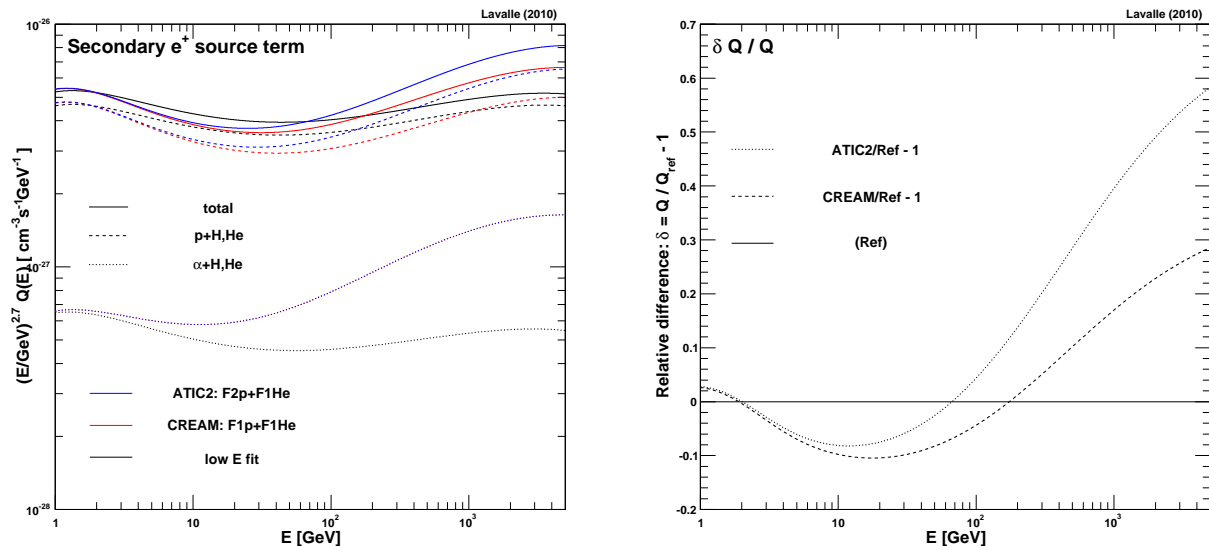


Figure 2. Left panel: Secondary positron source term for three different fit-based assumptions for the incident cosmic ray spectra; the contributions due to cosmic-ray protons (dashed curves) and α particles (dotted curves) are shown explicitly aside from the overall contributions (solid curves). Right panel: relative difference between the obtained overall source terms.

source terms at any energy. Therefore, the relative differences in flux predictions should be very close to the relative differences in the corresponding source terms, the latter being already plotted in the right panel of Fig. 2. This is actually verified in the right panel of Fig. 3, which can hardly be differentiated from the one previously mentioned, illustrating how efficient the approximation given in Eq. (4) is in this context. In the left panel of Fig. 3, we show the corresponding predictions for the secondary positron flux, which are derived with the *med* propagation parameters and with model M1 for the energy losses — these parameters can be found in Delahaye et al. (2010). From these plots, we readily conclude that the secondary positron flux prediction is affected over the whole GeV-TeV energy range, decreasing by $\sim 10\%$ below ~ 100 GeV, and increasing by more than 30% at TeV energies, up to 60% in the case of the ATIC2 cosmic ray fit. The spectral index is therefore increased accordingly by almost 2 digits, from ~ -3.5 to ~ -3.3 in the *med* case employed here.

For the sake of completeness, it is interesting to derive the theoretical uncertainty bands associated with these novel predictions, which come from the uncertainties in the propagation parameters. To this aim, we proceed as in Delahaye et al. (2009) by bracketing the *med* with the *min* and *max* propagation configurations. We report our results for the positron flux (fraction) in the top (bottom, respectively) panels of Fig. 4 — a solar modulation is applied, using the Force Field approximation (Gleeson & Axford 1968; Fisk 1971) with a Fisk potential of 600 MV, and ignoring any charge dependence effect potentially important below a few GeV (*e.g.* Heber & Potgieter 2006). The positron flux data are taken from Boezio et al. (2000); DuVernois et al. (2001); Aguilar et al. (2002), while the positron fraction data are from Barwick et al. (1997); Beatty et al. (2004); Aguilar et al. (2007); Adriani et al. (2010). To calculate

the positron fraction $f = \phi_{e^+}/(\phi_{e^+} + \phi_{e^-})$, we determined the denominator above 10 GeV from the Fermi-LAT data (Abdo et al. 2009; Fermi LAT collaboration 2010), and used the AMS01 data (Aguilar et al. 2002) to constrain the electron flux at lower energy. In all panels, we also display the result obtained by Moskalenko & Strong (1998), as fitted by Baltz & Edsjö (1998), since it is still very often used in the literature as a reference. Note that the predictions obtained from the low energy cosmic ray fit are obviously identical to the ones derived in Delahaye et al. (2010).

From the predictions based on the low energy cosmic ray fit to the ones based on the ATIC2 fit, the secondary positron spectrum is hardened, which translates into a slightly flatter positron fraction. Of course, we did not expect the present study to be relevant to the discussion on the rise of the positron fraction itself, since the enhancement in the secondary positron flux was already known to be by far too small from the incident cosmic-ray nuclei data. It is instead very useful so as to constrain any extra source of positrons, like pulsars or dark matter, with the data. Indeed, in that case, one needs to add a secondary contribution to the primary one in a consistent manner before comparing the sum to the data. From the top panels of Fig. 4, we note incidentally that the *min* propagation setup already leads to a conflict with the data because of its too small value of K_0 [see Eq. (4)] (associated with a small value of L , K_0/L being roughly fixed by secondary-to-primary cosmic-ray nuclei ratios). This configuration is in any case obsolete, since it is no longer supported by recent secondary-to-primary analyses (*e.g.* Putze et al. 2010), nor by the Fermi-LAT diffuse gamma-ray data (*e.g.* Abdo et al. 2010) (see also a dedicated discussion in Lavalle 2010). Nevertheless, it can still be thought of as an extreme configuration and used for illustration purposes.

We provide user-friendly empirical fitting functions associated with all these propagation models in Sec. 3.2.

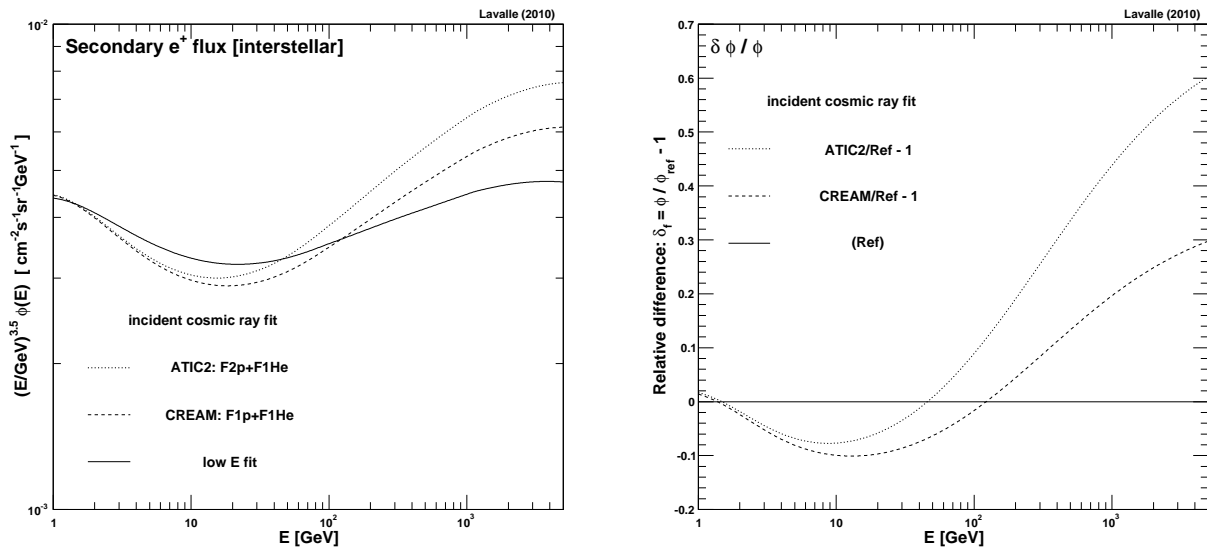


Figure 3. Left panel: Secondary positron flux predictions associated with the 3 different fit-based assumptions considered for the incident cosmic ray spectra; the *med* propagation setup has been used. Right panel: relative difference between the predictions shown in the left panel.

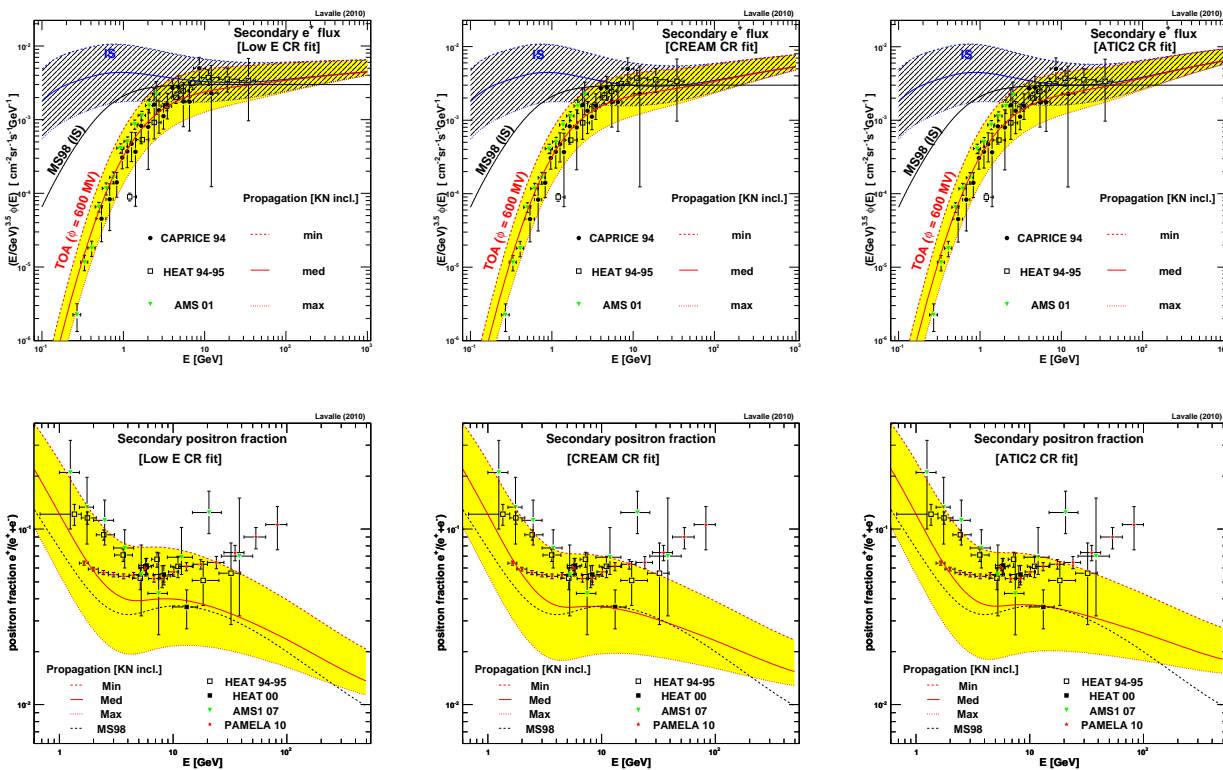


Figure 4. Top panels: secondary positron flux predictions, both interstellar (IS) and on top of atmosphere (TOA), assuming a Fisk potential of 600 MV for the solar modulation. Bottom panels: associated positron fractions. These predictions correspond to source terms calculated from either the low energy cosmic ray fit (left panels), the CREAM cosmic ray fit (middle panels), or the ATIC2 cosmic ray fit (right panels).

3 USER-FRIENDLY FITTING FORMULAE

In this section, we provide the reader with the parametric functions (i) that we used to fit the cosmic ray data and (ii) also the ones which fit our prediction results for the secondary positron flux.

3.1 Cosmic-ray proton and helium interstellar fluxes

The proton data can be accommodated by two different empirical functions, depending on whether one favors the CREAM (F1p) or ATIC2 (F2p) data at high energy. These functions are both characterized by the following parameterization:

$$\begin{aligned} \text{Fp}(E_k) &= \phi_p^0 \left[1 - e^{-\left(\frac{E_k}{E_{p1}}\right)^{p_1}} \right] \left[\frac{E_k}{10 \text{ GeV}/n} \right]^{-\gamma_p} \\ &\times \left[1 + \frac{E_k}{E_{p2}} \right]^{p_2} \left[1 + \frac{E_k}{E_{p3}} \right]^{p_3}. \end{aligned} \quad (5)$$

One recognizes a standard power law of main index γ_p associated with an exponential attenuation factor active at low energy, which clearly improves the low energy fit with respect to Eq. (3), and a double spectral correction of indices p_2 and p_3 operating above kinetic energies E_{p2} and E_{p3} , respectively. Note that function Fp behaves asymptotically as a power law of index $\gamma_\infty = -\gamma + p_2 + p_3$.

In contrast, a single function (F1He) is enough in the case of helium ions, since both sets of high energy data are in agreement. In that case, a slight correction to Eq. (3) is enough, so that

$$\text{FHe}(E_k/n) = \phi_\alpha^{\text{bess}}(E_k/n) \left[1 + \frac{\mathcal{R}}{\mathcal{R}_{p2}} \right]^{p_2} \left[1 + \frac{\mathcal{R}}{\mathcal{R}_{p3}} \right]^{p_3}, \quad (6)$$

where $\phi_\alpha^{\text{bess}}$ is given in Eq. (3), and \mathcal{R} is the rigidity. There is also a double spectral correction as in the case of protons. As function Fp, function FHe behaves asymptotically as a power law of index $\gamma_\infty = -b_2 + p_2 + p_3$, where b_2 is defined in Eq. (3).

Given the spread in the available data, we did not performed a χ^2 selection of the parameters. Indeed, this would require an *a priori* or expert selection of the data, which is beyond the scope of this paper. The values of the parameters used for functions F1p, F2p and F1He are listed in Table 1.

3.2 Secondary positron flux predictions

Here, we define an empirical function that provides a very good fit to the *interstellar* secondary positron flux predictions presented in Sec. 2.4:

$$\phi_{\text{fit}}(E) = \exp \left\{ \sum_{i=0} c_i \left[\ln \left(\frac{E}{\text{GeV}} \right) \right]^i \right\}. \quad (7)$$

The parameters associated with all the configurations discussed in Sec. 2.4 are given in Table 2. We emphasize that these parameters are valid only for the propagation models, energy loss configurations, and incident cosmic ray modelings discussed through this paper. These empirical fitting functions should not be used for other sets of parameters. They are valid from ~ 0.1 GeV to ~ 10 TeV.

4 CONCLUSION

In this paper, we have studied the impact of the spectral hardening observed in the cosmic-ray proton and helium fluxes by the ATIC2 (Panov et al. 2006, 2009) and CREAM (Ahn et al. 2010) experiments, on the secondary positron flux prediction. To this aim, we have revisited the calculation of the secondary positron source term, which spatially tracks the interstellar gas, showing that its energy distribution roughly scales like the incident cosmic ray spectrum. Because of the discrepancy in the proton fluxes observed by the CREAM and ATIC2 balloons — in contrast, both agree on the helium flux — we have considered two different cosmic ray modelings: one based on a fit to the CREAM proton data (moderate case), and another based on a fit to the ATIC2 proton data (maximal case), both using the same helium flux parameterization. The former (latter) case led to a 30% (60%, respectively) increase in the production rate of TeV positrons.

Then, we have propagated these positrons to the Earth, using the propagation framework described in Delahaye et al. (2010), which includes a fully relativistic treatment of the energy losses, with spatial diffusion parameters as constrained in Maurin et al. (2001), still consistent with the more recent analysis performed in Putze et al. (2010). We have notably explained why, in this context, the relative differences in the differential flux predictions were almost equal to the relative differences in the energy-dependent positron production rate, and consequently to the relative differences in the considered incident cosmic ray fluxes. This led us to establish a robust estimate of the effect: as for the positron production rate, the secondary positron flux is increased by up to 30% (60%) at TeV energies when constraining the cosmic-ray nuclei fluxes from the CREAM (ATIC2, respectively) data. Therefore, these predictions differs from the ones performed in Moskalenko & Strong (1998), Delahaye et al. (2009) and Delahaye et al. (2010), resulting in harder secondary positron spectra. We have also derived an estimate of the theoretical uncertainties. These results are complementary to the recent analysis of Donato & Serpico (2010) on the secondary antiproton and diffuse gamma-ray fluxes.

Finally, we have provided the reader with user-friendly parametric functions that allow to reproduce all the results derived in this paper, so that they can be straightforwardly exploited. For instance, one can use these functions to constrain any extra source of primary positrons against the existing (or forthcoming) data in a self-consistent way — in which case one needs to sum up the secondary and primary contributions. We again emphasize that these results are valid only in the frame of the propagation models described through the paper, so if used, one has to make sure that the same parameters are employed for the primary component.

ACKNOWLEDGEMENTS

We are grateful to T. Delahaye and P. Salati for interesting discussions about this study. This work was supported by the Spanish MICINNs Consolider-Ingenio 2010 Program under grant MultiDark CSD2009-00064. We also thank the support of the MICINN under grant FPA2009-08958, the Community of Madrid under grant HEPHACOS

	ϕ^0 [cm ⁻² s ⁻¹ GeV ⁻¹ sr ⁻¹]	α_p	E_{p1} [GeV]	p_1	E_{p2} [TeV]	p_2	E_{p3} [TeV]	p_3
F1p	3.09×10^{-3}	2.8	4	1.05	2.5	0.34	10	-0.29
F2p	3.09×10^{-3}	2.8	4	1.05	1.5	0.4	10	-0.35
F1He	-	-	-	-	1	0.5	10	-0.5

Table 1. Parameters used to fit the cosmic-ray proton (F1p, F2p) and helium (F1He) data, according to Eqs. (5) and (6). For function F1He, any parameter E_p (in GeV) in this table corresponds to \mathcal{R}_p (in GV) in the associated equation.

	Low E CRs			CREAM CRs			ATIC2 CRs		
	<i>min</i>	<i>med</i>	<i>max</i>	<i>min</i>	<i>med</i>	<i>max</i>	<i>min</i>	<i>med</i>	<i>max</i>
c_0	-4.61	-5.48	-6.4	-4.61	-5.48	-6.4	-4.41	-5.48	-6.4
c_1	-3.55	-3.486	-3.37	-3.6	-3.53	-3.41	-3.6	-3.53	-3.41
$c_2 (\times 10^{-2})$	-8.59	-8.34	-8.2	-9.28	-8.99	-8.83	-8.98	-8.68	-8.52
$c_3 (\times 10^{-2})$	2.21	2.16	2.13	2.73	2.67	2.64	2.79	2.73	2.69
$c_4 (\times 10^{-3})$	-1.41	-1.38	-1.37	-1.8	-1.77	-1.754	-1.88	-1.84	-1.82

Table 2. Parameters used to fit the interstellar secondary positron flux predictions, from Eq. (7).

S2009/ESP-1473, and the European Union under the Marie Curie-ITN program PITN-GA-2009-237920.

REFERENCES

- Abdo, A. A., Ackermann, M., Ajello, M., & Atwood, W. B. 2010, ArXiv e-prints [arXiv:1011.0816]
- Abdo, A. A., Ackermann, M., Ajello, M., et al. 2009, Physical Review Letters, 102, 181101
- Adriani, O., Barbarino, G. C., Bazilevskaya, G. A., et al. 2010, Astroparticle Physics, 34, 1
- Adriani, O., Barbarino, G. C., Bazilevskaya, G. A., et al. 2009, Nature, 458, 607
- Aguilar, M., Alcaraz, J., Allaby, J., et al. 2002, Phys. Rept., 366, 331
- Aguilar, M., Alcaraz, J., Allaby, J., et al. 2007, Physics Letters B, 646, 145
- Aharonian, F. A., Atoyan, A. M., & Voelk, H. J. 1995, Astron. Astroph., 294, L41
- Ahn, H. S., Allison, P., Bagliesi, M. G., et al. 2010, Astrophys. J. Lett., 714, L89
- Baltz, E. A. & Edsjö, J. 1998, Phys. Rev. D, 59, 023511
- Barwick, S. W., Beatty, J. J., Bhattacharyya, A., et al. 1997, Astrophys. J. Lett., 482, L191+
- Beatty, J. J., Bhattacharyya, A., Bower, C., et al. 2004, Physical Review Letters, 93, 241102
- Berezhko, E. G., Ksenofontov, L. T., Ptuskin, V. S., Zirakashvili, V. N., & Völk, H. J. 2003, Astron. Astroph., 410, 189
- Berezinskii, V. S., Bulanov, S. V., Dogiel, V. A., & Ptuskin, V. S. 1990, Astrophysics of cosmic rays (Amsterdam: North-Holland, 1990, edited by Ginzburg, V.L.)
- Blasi, P. 2009, Physical Review Letters, 103, 051104
- Boezio, M., Bonvicini, V., Schiavon, P., et al. 2003, Astroparticle Physics, 19, 583
- Boezio, M., Carlson, P., Francke, T., et al. 1999, Astrophys. J., 518, 457
- Boezio, M., Carlson, P., Francke, T., et al. 2000, Astrophys. J., 532, 653
- Boulares, A. 1989, Astrophys. J., 342, 807
- Chi, X., Cheng, K. S., & Young, E. C. M. 1996, Astrophys. J. Lett., 459, L83+
- Delahaye, T., Donato, F., Fornengo, N., et al. 2009, Astron. Astroph., 501, 821
- Delahaye, T., Lavalle, J., Lineros, R., Donato, F., & Fornengo, N. 2010, ArXiv e-prints [arXiv:1002.1910]
- Donato, F., Fornengo, N., Maurin, D., Salati, P., & Taillet, R. 2004, Phys. Rev. D, 69, 063501
- Donato, F. & Serpico, P. D. 2010, ArXiv e-prints [arXiv:1010.5679]
- DuVernois, M. A., Barwick, S. W., Beatty, J. J., et al. 2001, Astrophys. J., 559, 296
- Fermi LAT collaboration. 2010, ArXiv e-prints [arXiv:1008.3999]
- Ferrière, K. M. 2001, Reviews of Modern Physics, 73, 1031
- Fisk, L. A. 1971, J. Geophys. Res., 76, 221
- Ginzburg, V. L. & Syrovatskii, S. I. 1964, The Origin of Cosmic Rays (The Origin of Cosmic Rays, New York: Macmillan, 1964)
- Gleeson, L. J. & Axford, W. I. 1968, Astrophys. J., 154, 1011
- Haino, S., Sanuki, T., Abe, K., et al. 2004, Physics Letters B, 594, 35
- Harding, A. K. & Ramaty, R. 1987, in International Cosmic Ray Conference, Vol. 2, International Cosmic Ray Conference, 92–+
- Heber, B. & Potgieter, M. S. 2006, Space Science Rev., 127, 117
- Kamae, T., Karlsson, N., Mizuno, T., Abe, T., & Koi, T. 2006, Astrophys. J., 647, 692
- Lavalle, J. 2010, Phys. Rev. D, 82, 081302
- Longair, M. S. 1994, High energy astrophysics. Vol.2: Stars, the galaxy and the interstellar medium (Cambridge: Cambridge University Press, —c1994, 2nd ed.)
- Malyshev, D., Cholis, I., & Gelfand, J. 2009, Phys. Rev. D, 80, 063005

- Maurin, D., Donato, F., Taillet, R., & Salati, P. 2001, *Astrophys. J.*, 555, 585
- Moskalenko, I. V. & Strong, A. W. 1998, *Astrophys. J.*, 493, 694
- Norbury, J. W. & Townsend, L. W. 2007, *Nuclear Instruments and Methods in Physics Research B*, 254, 187
- Panov, A. D., Adams, J. H., Ahn, H. S., et al. 2006, *ArXiv Astrophysics e-prints* [arXiv:astro-ph/0612377]
- Panov, A. D., Adams, J. H., Ahn, H. S., et al. 2009, *Bulletin of the Russian Academy of Science, Phys.*, 73, 564
- Profumo, S. 2008, *ArXiv e-prints* [arXiv:0812.4457]
- Putze, A., Derome, L., & Maurin, D. 2010, *Astron. Astroph.*, 516, A66+
- Roberts, J. P. 2010, *ArXiv e-prints* [arXiv:1005.4668]
- Sanuki, T., Motoki, M., Matsumoto, H., et al. 2000, *Astrophys. J.*, 545, 1135
- Shaviv, N. J., Nakar, E., & Piran, T. 2009, *Physical Review Letters*, 103, 111302
- Shen, C. S. 1970, *Astrophys. J. Lett.*, 162, L181+
- Shikaze, Y., Haino, S., Abe, K., et al. 2007, *Astroparticle Physics*, 28, 154
- Sturrock, P. A. 1970, *Nature*, 227, 465
- Taillet, R. & Maurin, D. 2003, *Astron. Astroph.*, 402, 971
- Wang, J. Z., Seo, E. S., Anraku, K., et al. 2002, *Astrophys. J.*, 564, 244
- Yüksel, H., Kistler, M. D., & Stanev, T. 2009, *Physical Review Letters*, 103, 051101